AIP Advances

Correlation between Pd metal thickness and thermally stable perpendicular magnetic anisotropy features in $[Co/Pd]_n$ multilayers at annealing temperatures up to 500 °C

Cite as: AIP Advances **5**, 027137 (2015); https://doi.org/10.1063/1.4913997
Submitted: 16 November 2014 • Accepted: 20 February 2015 • Published Online: 27 February 2015

Gwang Guk An, Ja Bin Lee, Seung Mo Yang, et al.

View Online Export Citation CrossMark

ARTICLES YOU MAY BE INTERESTED IN

Perpendicular magnetic anisotropy in Pd/Co thin film layered structures
Applied Physics Letters **47**, 178 (1985); https://doi.org/10.1063/1.96254

Perpendicular magnetic anisotropy in Pd/Co and Pt/Co thin-film layered structures
Journal of Applied Physics **63**, 5066 (1988); https://doi.org/10.1063/1.340404

The design and verification of MuMax3
AIP Advances **4**, 107133 (2014); https://doi.org/10.1063/1.4899186

AIP Publishing

© 2015 Author(s).

Correlation between Pd metal thickness and thermally stable perpendicular magnetic anisotropy features in $[Co/Pd]_n$ multilayers at annealing temperatures up to 500 °C

Gwang Guk An,[1] Ja Bin Lee,[1] Seung Mo Yang,[1] Jae Hong Kim,[2]
Woo Seong Chung,[3] Kap Soo Yoon,[1] and Jin Pyo Hong[1,2,a]
[1]*Novel Functional Materials and Devices Lab, The Research Institute for Natural Science, Department of Physics, Hanyang University, Seoul 133-791, South Korea*
[2]*Division of Nano-Scale Semiconductor Engineering, Hanyang University, Seoul 133-791, South Korea*
[3]*Nano Quantum Electronics Lab, Department of Electronics and Computer Engineering, Hanyang University, Seoul 133-791, South Korea*

(Received 16 November 2014; accepted 20 February 2015; published online 27 February 2015)

We examine highly stable perpendicular magnetic anisotropy (PMA) features of $[Co/Pd]_{10}$ multilayers (MLs) versus Pd thickness at various ex-situ annealing temperatures. Thermally stable PMA characteristics were observed up to 500 °C, confirming the suitability of these systems for industrial applications at this temperature. Experimental observations suggest that the choice of equivalent Co and Pd layer thicknesses in a ML configuration ensures thermally stable PMA features, even at higher annealing temperatures. X-ray diffraction patterns and cross-sectional transmission electron microscopy images were obtained to determine thickness, post-annealing PMA behavior, and to explore the structural features that govern these findings. © *2015 Author(s). All article content, except where otherwise noted, is licensed under a Creative Commons Attribution 3.0 Unported License.* [http://dx.doi.org/10.1063/1.4913997]

I. INTRODUCTION

Perpendicular spin-transfer torque magnetic random access memories (p-STT MRAMs) have garnered considerable interest as alternatives to conventional memories due to a fast write time of ~10 ns, non-volatile memory characteristics, and extremely low power consumption.[1–3] However, one goal in the development of p-STT-MRAMs beyond a feature size of 20 nm is to meet the demands of device performance, including a high tunneling magnetoresistance ratio (TMR) of 150%, a low critical current density (J_C) of 4.7 MA/cm^2, and a good thermal stability ($\Delta = E/k_BT$) of 74. Here, $E = K_{eff}V$ is the energy barrier, M_S is the saturation magnetization, H_k is the anisotropy field, K_{eff} is the effective perpendicular magnetic anisotropy (PMA) energy density, V is the volume of the magnetic layer, k_B is the Boltzmann constant, and T is temperature.[3,4] In particular, a perpendicular magnetic tunnel junction (p-MTJ) suitable for PMA characteristics is a key factor to obtain a low J_C and a high thermal stability, which cannot be achieved with in-plane MTJ (i-MTJ).[3]

A variety of PMA systems including an $L1_0$ alloy, multilayers (MLs), and rare earth-transition metal (RE-TM) alloys have been extensively employed to yield outstanding PMA performance.[5–8] Among them, artificial ML matrices composed of ferromagnetic and noble metals, such as Co/Pd, Co/Pt, Fe/Pd, and Fe/Pt, have shown that ML matrices are promising candidates for use in p-MTJs.[4,9–12] Alternating two ultra-thin layers with different thicknesses in the ML matrix permits appreciable tuning of magnetic characteristics and yields strong PMA features. These PMA properties may originate from possible interface spin-orbit coupling between ferromagnetic/noble metals.[13,14] However, one hurdle still remains to improve the PMA characteristics in a ML matrix,

[a]Author to whom correspondence should be addressed; electronic mail: jphong@hanyang.ac.kr

 ©Author(s) 2015

namely, limited annealing stability.[11,12] The low annealing stability of PMA properties may be related to unknown structural stress or interfaces between ferromagnetic and metal layers. Therefore, much effort has been dedicated towards ensuring annealing stability in *p*-MTJs that can be operated at more than 400°C for a wide range of applications, such as high-density and low-power p-STT MRAM devices.[3]

Therefore, in this letter, we present the correlation between Pd metal thickness and PMA features of [Co/Pd] MLs at annealing temperatures ranging from 200 to 500°C. The Pd thickness was varied from 0.1 to 0.9 nm to achieve thermally stable features at a fixed Co thickness. The magnetic and structural characteristics were analyzed by utilizing vibrating sample magnetometer (VSM), X-ray diffraction (XRD), and high-resolution transmission electron microscopy (HR-TEM) systems. In order to clarify Pd thickness-dependent structural characteristics under various annealing temperatures, the structural features underlying the experimental findings are discussed.

II. EXPERIMENTAL

Various samples with a stack sequence of Ta (3)/Ru (5)/Pd (3)/[Co(t_{Co})/Pd (t_{Pd})]$_{10}$/Pd (3) were prepared on a thermally-oxidized Si substrate, where the numbers in parentheses reflect the nominal thickness in nanometers. A Ta/Ru/Pd seed layer was selected for crystal orientation in this work. Dual DC and RF magnetron sputtering systems with a base pressure below 2×10^{-8} Torr were used for the growth of all samples. The thickness of Pd (t_{Pd}) was varied from 0.1 to 0.9 nm with fixed Co layers of 0.1, 0.2, and 0.3 nm in thickness. In this work, the [Co (0.1)/Pd (t_{Pd})]$_{10}$, [Co (0.2)/Pd (t_{Pd})]$_{10}$, and [Co (0.3)/Pd (t_{Pd})]$_{10}$ samples with 0.1, 0.2, and 0.3 nm thick Co layers are referred to as the 0.1, 0.2, and 0.3 series, respectively. All samples were annealed at different temperatures ranging from 200 to 500°C under a 30-kOe magnetic field for an hour, where the base pressure in the annealing system was below 10^{-6} Torr. The effective PMA energy density (K_{eff}) was estimated from the enclosed area of the *M*-*H* curves measured using a VSM between the out-of-plane and in-plane hysteresis loops with respect to the sample plane, where *M* and *H* represent magnetization and applied magnetic field, respectively.[9,10]

III. RESULTS AND DISCUSSION

The dependence of K_{eff} on the Pd thickness of three different series is plotted in Figure 1, in which the annealing temperatures were at first varied from 200 to 350 °C. All the samples showed

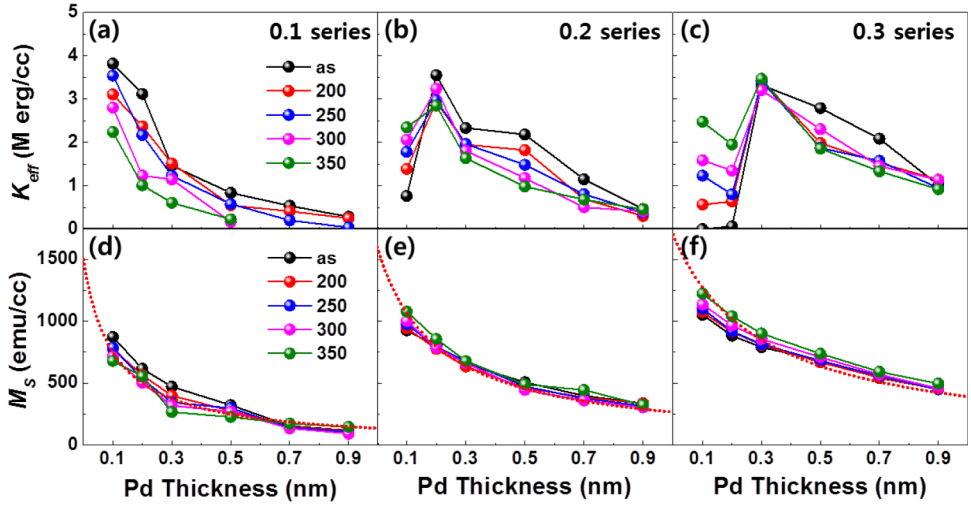

FIG. 1. Effective magnetic anisotropy (K_{eff}) and saturation magnetization (M_S) of 0.1 (a, d), 0.2 (b, e), and 0.3 (c, f) series samples as a function of Pd thickness. The annealing temperatures were varied from an as-grown state to 350 °C. As determined from the summarized curves, an enhanced K_{eff} appears at an equivalent thickness (dashed lines) of Co and Pd layers in all sample series, regardless of annealing temperatures.

a magnetic easy axis direction normal to the sample plane, demonstrating the presence of enhanced PMAs up to 350 °C in our ML matrix (not shown in this figure). Figure 1(a) reveals the summarized K_{eff} of [Co (0.1)/Pd (t_{Pd})]$_{10}$, i.e., the "0.1 series." As seen from this figure, the maximum K_{eff} of 3.8 Merg/cc was obtained at t_{Pd} = 0.2 nm in the as-deposited state (black dots). An increase in annealing temperature (T_a) causes a rapid reduction in the K_{eff}. In particular, at T_a = 350°C (green dots), the maximum K_{eff} was 2.3 Merg/cc at t_{Pd} = 0.1 nm, suggesting that similar Co and Pd thicknesses are required for annealing stability. For the 0.2 series, the maximum K_{eff} of 3.7 Merg/cc was observed at t_{Pd} = 0.2 nm in the as-deposited states, and decreased to 2.9 Merg/cc nm under T_a = 350 °C, as shown in Fig. 1(b). For the 0.3 series, a similar trend with respect to t_{pd} was revealed. The t_{pd} = 0.3 nm thickness showed a maximum K_{eff} of 3.6 Merg/cc at T_a = 350 °C, as shown in Fig. 1(c). Thus, these experimental findings demonstrate that high annealing stability is achieved when the same thickness is chosen for both Co and Pd layers in the MLs. Figures 1(d), 1(e), and 1(f) display the saturation magnetization (M_S) with increasing Pd thickness in each series. The M_S value increases as the Co thickness increases. The red dotted lines in each figure represent the equation $M_S = M_0 \cdot t_{Co}/(t_{Co} + t_{Pd})$, where the M_0 is the saturation magnetization limit when the Pd thickness is zero. The M_0 values were estimated to be 1500, 1600, and 1700 emu/cc for the 0.1, 0.2, and 0.3 series, respectively. These M_0 values are large compared with the bulk M_S value for Co (~1400 emu/cc), which seems to originate from the Co orbital moment contribution.[11] In particular, compared with those of the 0.2 and 0.3 series, the magnetic properties of all 0.1 series samples deteriorated as the annealing temperature increased, as shown in Figs. 1(a) and 1(d). In general, the origin of PMA is expected to result from spin-orbit coupling at the clean interface between ferromagnetic and non-magnetic materials. However, the thin Co layer in the 0.1 series is highly susceptible to surface damage during sputtering of the upper Pd layer, as demonstrated for other Co/Pt ML configurations.[11–14] On the other hand, the 0.2 and 0.3 series with thicker Co layers are more tolerant of the sputtering influence of the upper Pd layer. As a result, the saturation magnetization of the 0.2 and 0.3 series increases as annealing temperature increases, as shown in Figs. 1(e) and 1(f).

Figure 2 shows the representative in-plane (black squares) and out-of-plane (red circles) normalized M-H loops of four as-deposited and annealed samples: [(t_{Co},t_{Pd}) = (0.2,0.2: Sample A), (0.2,

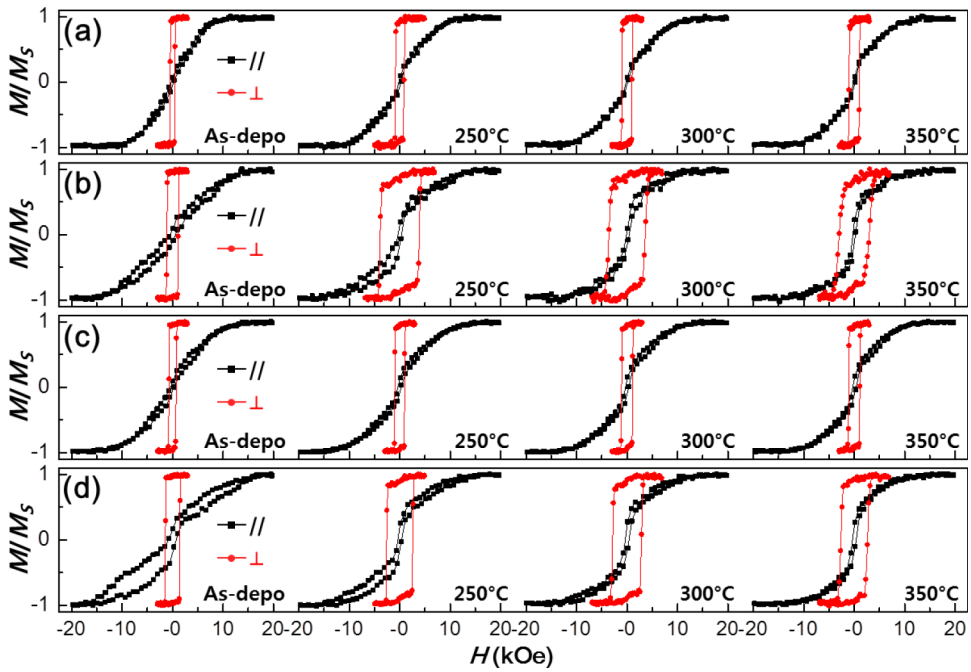

FIG. 2. Normalized in-plane (black) and out-of-plane (red) M-H hysteresis loops of Samples (a) A (0.2,0.2), (b) B (0.2, 0.5), (c) C (0.3, 0.3), and (d) D (0.3. 0.7) annealed at temperatures ranging from as-deposited to 350 °C for an hour under 3 Tesla. The M-H behaviors of Samples B and D reveal the relatively enhanced H_C and deteriorated PMA features with an increase in annealing temperature.

0.5: Sample B), (0.3, 0.3: Sample C), and (0.3, 0.7: Sample D)]. The H-field was scanned from -20 to 20 kOe. The samples tested here exhibited two types of behavior, which differed slightly in the remanence ratio and in-plane saturation field (H_K). Figures 2(a) and 2(c) exhibit the relatively stable PMA features of Samples A and C, which have equivalent Co and Pd thicknesses. An increase in annealing temperature up to 350 °C did not affect the remanence ratio and H_K significantly for Samples A and C. In contrast, as shown in Figs. 2(b) and 2(d), the remanence ratio and H_K of samples B and D were reduced from about 97 % to ~80 % and from 14 kOe to 10 kOe at T_a = 350 °C, respectively. The reduction of H_K results in a small K_{eff} value during annealing, as shown in Figs. 2(b) and 2(d). In addition, the remarkable variation in coercive field (H_C) with annealing temperature in Samples B and D indicates the possibility of structural instability.[15]

Thus, in order to further validate the structural variation in the MLs, HR-XRD analyses of as-grown and annealed Samples A, B, C, and D at 350 °C were conducted. The results are shown in Figure 3. All the samples exhibited a (111) crystal orientation normal to the film plane in the 2θ region around 40°. However, as shown in Fig. 3(a), as-grown Samples A and C showed rather broad and low intensity peaks at around 40.65° (black dashed line) and 40.90° (blue dashed line), respectively, along with shoulder peaks that were normally detected in MLs. In addition, a relatively larger Co content initially present in Sample C provided a larger 2θ angle than Sample A. Samples B and D containing thick Pd layers revealed peak shifts toward lower angles of around 40.43° (red dashed line). These peak shifts are likely due to the crystal lattice expansion of the [Co/Pd] multilayer in

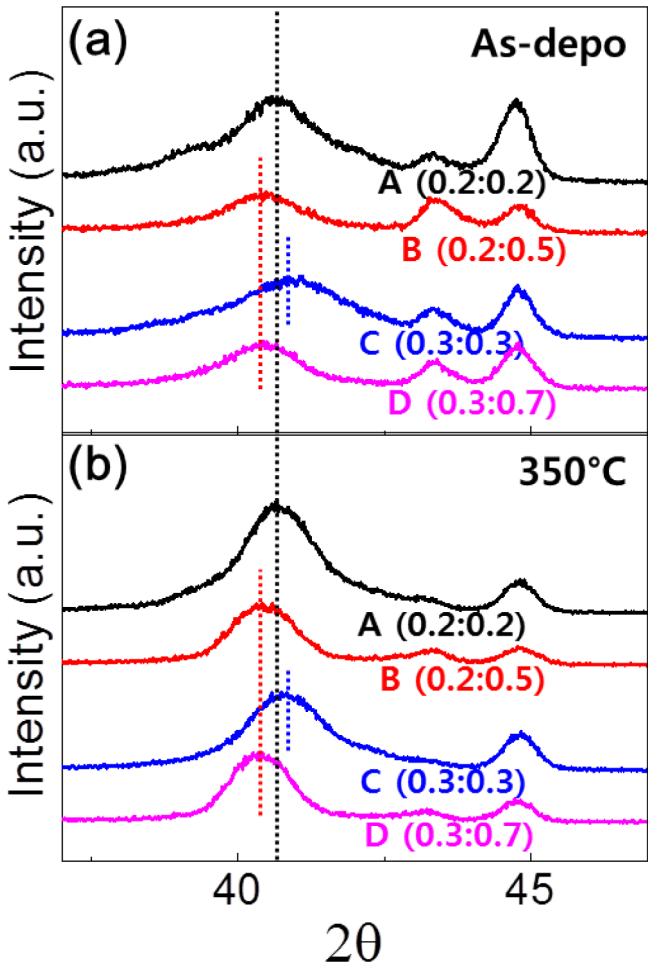

FIG. 3. Out-of-plane XRD θ-2θ patterns for Samples A (0.2, 0.2; black), B (0.2, 0.5; red), C (0.3, 0.3; blue), and D (0.3, 0.7; pink) in (a) as-deposited state and (b) annealed at 350 °C.

order to match the lattice of the Pd layer. Annealing at 350 °C revealed sharp and strong CoPd (111) peak intensities without showing the presence of shoulder peaks and shifts, as shown in Fig. 3(b). These observations may reflect the presence of an alloy-like phase arising from atomic intermixing after annealing.

Since the MLs containing the same thicknesses of Co and Pd revealed highly promising PMA stability, further higher annealing ranging from 450 to 500 °C was also conducted. Figure 4 shows the individual *M*-*H* curves and out-of-plane XRD peaks of Samples A, B, C, and D after annealing. The PMA properties of Samples A and C (Figs. 4(a) and 4(c), respectively) remained up to 450 °C, and K_{eff} values of 3.28 Merg/cc and 2.95 Merg/cc were maintained for Samples A and C after 500 °C annealing, respectively. However, samples B and D (Figs. 4(b) and 4(d), respectively) deteriorated at 450 °C, reflecting deteriorated PMA features. On the other hand, XRD analyses for all the annealed samples (Figs. 4(e) and 4(f)) indicated enhanced peaks without significantly exhibiting peak shifts compared with those of as-deposited samples. Therefore, we expect that higher annealing stability might be governed by initial structural formation that will be discussed later.

Since annealing stability strongly relies on structural characteristics,[4,7,11] more structural investigations were carried out. Figure 5(a) reveals rocking curves with the corresponding full-width at half-maximum (FWHM) for each CoPd (111) orientation for Samples A, B, C, and D in the as-deposited state and after annealing at 500 °C. Samples A and C displayed better crystal orientation qualities than Samples B and D in the as-deposited state. These initial as-grown structural enhancement of Samples A and C were also maintained even in annealed states. When as grown Samples B and C were compared, the structural features seemed to be similar to each other, but the PMA characteristics of Samples B and C were strongly affected after annealing process, as shown in Figs. 1(b) and 1(c). Thus, since it is widely believed that the Co/Pd intermixing or Pd diffusion is one of the main factors for PMA degradation during annealing process,[16] we expect that the PMA degradation of Sample B under annealing may arise from the easy Co/Pd intermixing event or Pd diffusion phenomenon from the buffer and capping layers due to the similar lattice constants between the [Co/Pd] MLs and the Pd buffer/or capping layer. However, equivalent Co and Pd thicknesses used in the MLs may suppress the atomic intermixing or Pd diffusion event

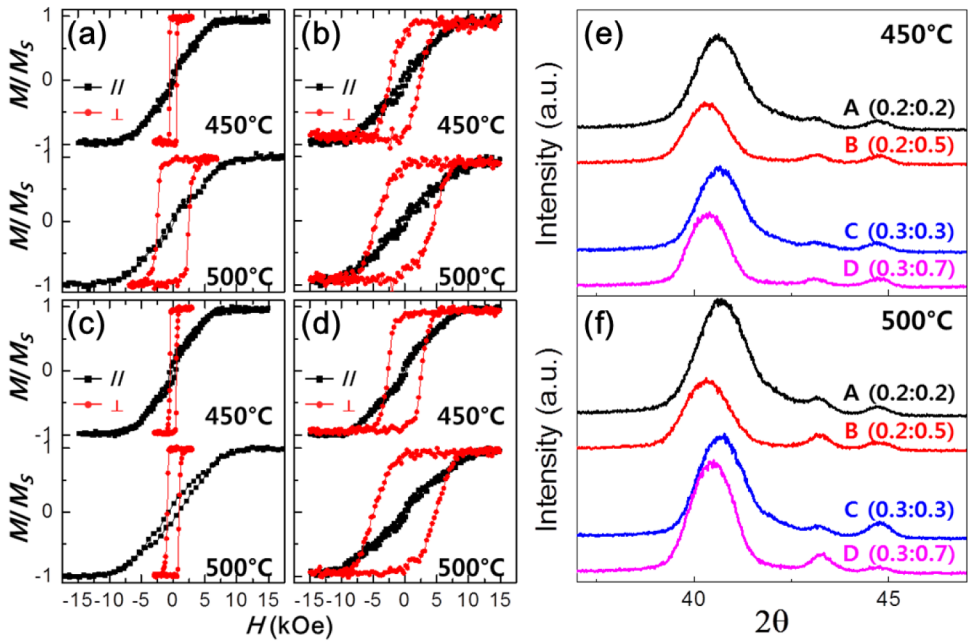

FIG. 4. *M*-*H* hysteresis curves of Samples (a) A (0.2,0.2), (b) B (0.2, 0.5), (c) C (0.3, 0.3), and (d) D (0.3. 0.7) annealed at 450 °C (top) and 500 °C (bottom) displaying the clear appearance of PMA characteristics. XRD patterns for each samples annealed at (e) 450 °C and (f) 500 °C.

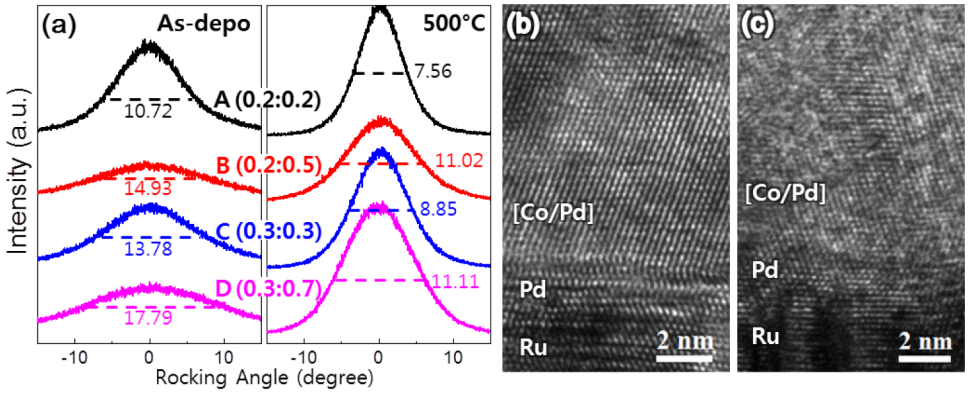

FIG. 5. (a) Rocking curve plots of Samples A (0.2,0.2), B (0.2, 0.5), C (0.3, 0.3), and D (0.3. 0.7) measured along the CoPd (111) orientation for an as-deposited sample and a sample annealed at 500 °C. Cross-sectional TEM images of (b) Sample C (0.3,0.3) and (c) Sample D (0.3, 0.7) annealed at 500 °C.

under annealing, resulting in the preservation of PMA behavior up to 500 °C in Sample C. Figures 5(b) and 5(c) show the TEM analyses for Samples C and D annealed at 500 °C, respectively. As seen in these figures, Sample C showed a single-like alloy phase, while Sample D exhibited poly-crystalline properties with clear grain boundaries. Furthermore, interfaces between the CoPd and Pd seed/capping layers in Sample D were not clearly observed, while clear interfaces between them were obtained in Sample C. The above structural observations suggest that the [Co/Pd] MLs containing a thick Pd layer was highly susceptible to low annealing stability. The relationship between the annealing temperature and magnetic/structural features of Co/Pd MLs still remains a challenge since our results are inconsistent with the observations of other groups, in which different Co and Pd thicknesses were frequently used in the MLs.[4,14,16] Therefore, more detailed studies are necessary to clarify the structural characteristics in ML configurations.

IV. CONCLUSIONS

In conclusion, we report thermally stable PMA features of Co/Pd MLs exhibiting 3 Merg/cc even after 500 °C annealing, reflecting a highly promising candidate for the realization of high performance devices. Structural and magnetic features were systematically examined, along with a structural nature that can possibly develop under annealing. Our experimental observations suggest the use of the same Co/Pd thickness in a [Co/Pd] ML for higher PMA features. The reason for improvement in PMA features was possibly the presence of an alloy-like-ordered structure by suppressing atomic intermixing and Pd diffusion during annealing. We anticipate that the ability to improve the PMA performance even at a higher annealing temperature will meet the demands of stable STT-MRAM devices.

ACKNOWLEDGMENTS

This research was supported by a grant from the National Research Foundation of Korea (NRF) funded by the Ministry of Education (NRF-2013R1A1A2060350).

[1] T. Kawahara, R. Takemura, K. Miura, J. Hayakawa, S. Ikeda, Y. M. Lee, R. Sasaki, Y. Goto, K. Ito, T. Meguro, F. Matsukura, H. Takahashi, H. Matsuoka, and H. Ohno, IEEE J. Solid-State Circuits **43**, 109 (2008).
[2] R. Takemura, T. Kawahara, K. Miura, H. Yamamoto, J. Hayakawa, N. Matsuzaka, K. Ono, M. Yamanouchi, K. Ito, H. Takahashi, S. Ikeda, H. Hasegawa, H. Matsuoka, and H. Ohno, IEEE J. Solid-State Circuits **45**, 869 (2010).
[3] T. Kawahara, K. Ito, R. Takemura, and H. Ohno, Microelectronics Reliability **52**, 613 (2012).
[4] K. Yakushiji, T. Saruya, H. Kubota, A. Fukushima, T. Nagahama, S. Yuasa, and K. Ando, Appl. Phys. Lett. **97**, 232508 (2010).
[5] T. Moriyama, S. Mitani, T. Seki, T. Shima, K. Takanashi, and A. Sakuma, J. Appl. Phys. **95**, 6789 (2004).
[6] M. Yoshikawa, E. Kitagawa, T. Nagase, T. Daibou, M. Nagamine, K. Nishiyama, T. Kishi, and H. Yoda, IEEE Trans. Magn. **44**, 2573 (2008).

[7] G. M. Choi, B. C. Min, and K. H. Shin, Appl. Phys. Lett. **97**, 202503 (2010).
[8] Q. L. Ma, T. Kubota, S. Mizukami, X. M. Zhang, H. Naganuma, M. Oogane, Y. Ando, and T. Miyazaki, Appl. Phys. Lett. **101**, 032402 (2012).
[9] J. H. Jung, S. H. Lim, and S. R. Lee, J. Nanosci. Nanotechnol. **11**, 6233 (2011).
[10] S. Ishikawa, H. Sato, M. Yamanouchi, S. Ikeda, S. Fukami, F. Matsukura, and H. Ohno, J. Appl. Phys. **113**, 17C721 (2013).
[11] M. Gottwald, K. Lee, J. J. Kan, B. Ocker, J. Wrona, S. Tibus, J. Langer, S. H. Kang, and E. E. Fullerton, Appl. Phys. Lett. **102**, 052405 (2013).
[12] N. Nakajima, T. Koide, T. Shidara, H. Miyauchi, H. Fukutani, A. Fujimori, K. Iio, T. Katayama, M. Nývlt, and Y. Suzuki, Phys. Rev. Lett. **81**, 5229 (1998).
[13] P. Kamp, A. Marty, B. Gilles, R. Hoffmann, S. Marchesini, M. Belakhovsky, C. Boeglin, H. A. Dürr, S. S. Dhesi, G. van der Laan, and A. Rogalev, Phys. Rev. B **59**, 1105 (1999).
[14] T. Y. Lee, D. S. Son, S. H. Lim, and S. R. Lee, J. Appl. Phys. **113**, 216102 (2013).
[15] E. P. Sajitha, J. Walowski, D. Watanabe, S. Mizukami, F. Wu, H. Naganuma, M. Oogane, Y. Ando, and T. Miyazaki, IEEE Trans. Magn. **46**, 2056 (2010).
[16] G. Hu, T. Topuria, P. M. Rice, Jean Jordan-Sweet, and D. C. Worledge, IEEE Magn. Lett. **4**, 3000104 (2013).